

## Wear detection of brass bond diamond grinding wheel by spectral coherence of grinding forces

Bin Dong, Christian Vogt, Rolf Rascher

Laboratory of Optical Engineering, Technische Hochschule Deggendorf, Edlmairstraße 6 & 8, 94469 Deggendorf, German

[sagittarius1013@gmail.com](mailto:sagittarius1013@gmail.com)

### Abstract

Wear detection for grinding wheel is a key problem in abrasive process. Integrated product of spectral coherence (IPSCoh), as a derivative of spectral correlation, is introduced to extract features from tangential and normal grinding forces and then to evaluate the wheel wear status. To verify the performance of IPSCoh, a grinding system is established to grind a round flat silica carbide workpiece and the generated grinding forces are measured by a Kistler dynamometer. The integrated products of spectral coherences of the two grinding forces both show that the force signals not only have abundant harmonics, but also present strong second-order cyclostationarity. More important, the wear flat length of the grinding wheel can be estimated by specific peaks in the IPSCoh in each grinding pass.

Wear detection, brass bond diamond grinding wheel, grinding force, spectral correlation, spectral coherence, cyclostationarity

### 1. Introduction

Grinding wheel wear, as one of key problems in grinding, has been investigated for long time [1]. Its detection is still the hot topic in mechanical manufacturing. Many advanced sensors are applied to record process signals, e.g. force, acoustic emission, and power, produced in grinding [2]. Relative to the utilization of the powerful sensors, few advanced signal processing methods are taken to study the measured process signals. Popular but simple methods, for example spectral analysis, can only provide limit information for the wear detection of grinding wheel [3]. Their reliability cannot fully meet the requirements from industrial applications.

Spectral correlation, as a powerful tool in cyclostationary analysis, has obtained great success in fault diagnosis of rotating machinery [4]. Grinding wheel belongs to the rotating machinery. One question naturally emerges: can the spectral correlation detect the wear – a normal “fault” of the grinding wheel via the measured grinding forces?

The rest of the paper is contributed to answer the above question. Section 2 briefly discusses the theory of spectral correlation. Grinding experiment is introduced in Section 3. Section 4 concentrates on the analysis of measured grinding forces for the wheel wear detection, especially by using spectral coherence. Two conclusions are made in last section.

### 2. Spectral coherence of grinding forces

Tangential and normal forces are more sensitive to grinding wheel wear than axial force. Thus only the former two are taken into account in the following discussion.

As introduced by W. A. Gardner in [5], the spectral correlation of a measured (tangential or normal) grinding force  $x(t)$  with length  $\Delta t$  can be formulized as

$$S_x^\alpha(f) = \lim_{\Delta f \rightarrow 0} \lim_{\Delta t \rightarrow \infty} \frac{1}{\Delta t} \int_{-\Delta t/2}^{\Delta t/2} \Delta f X_{1/\Delta f}(t, f + \alpha/2) X_{1/\Delta f}^*(t, f - \alpha/2) dt, \quad (1)$$

where  $\alpha$  and  $f$  denote cyclic frequency and spectral frequency, respectively, and the superscript \* symbolizes the conjugate operation. The variable  $X_{1/\Delta f}(t, f)$  stands for the short-time Fourier transform of the grinding force signal  $x(t)$ . Thus Eq. (1) measures the correlation degree between two conjugate spectral components at the frequencies  $f + \alpha/2$  and  $f - \alpha/2$ .

To get rid of the limit of amplitude difference in the spectral components, one derivative of the spectral correlation, named as integrated product of spectral coherence (IPSCoh), is applied here to extract the wheel wear information from the grinding forces. IPSCoh is first introduced in [6], and its value in the spectral frequency band  $[f_1, f_2]$  is calculated by

$$IPSCoh_{f_1}^{f_2}(\alpha) = \int_{f_1}^{f_2} \frac{S_x^\alpha(f + \frac{\alpha}{2})}{\sqrt{|S_x(f + \frac{\alpha}{2}) S_x^*(f)|}} \frac{S_x^\alpha(f - \frac{\alpha}{2})}{\sqrt{|S_x(f - \frac{\alpha}{2}) S_x^*(f)|}} df, \quad (2)$$

where  $S_x(f)$  is the power spectral density of the signal  $x(t)$ .

### 3. Experiment configuration

To demonstrate the performance of IPSCoh for the wheel wear detection, a laboratory experiment was set up. Figure 1 shows the full configuration of the grinding experiment.

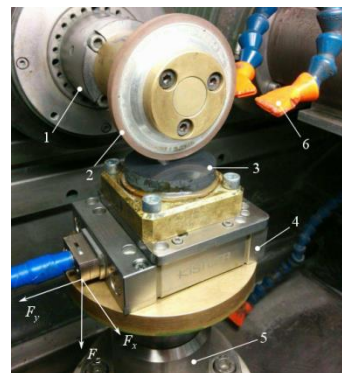


Figure 1. Configuration of grinding experiment: 1 - spindle, 2 - brass bond diamond grinding wheel, 3 - SiC workpiece, 4 - Kistler dynamometer, 5 - workpiece spindle, and 6 - nozzle.

A brass bond diamond grinding wheel with diameter 95 mm and grain size D15 was used to grind one round flat silica carbide (SiC) workpiece with diameter 50 mm, which was implemented on a high precision machine tool – ASM100 CNC-TC. The applied grinding parameters are: spindle speed 2600 rpm, depth of cut 12  $\mu\text{m}$ , and feed rate 1275 mm/min. Meanwhile, the traverse feed was set as 0.1 mm between each two grinding tracks in  $F_x$  direction (see Fig. 1).

Four grinding passes were conducted to guarantee it that noticeable wear is produced on the brass bond diamond grinding wheel. In each grinding pass, a Kistler dynamometer 9256C was triggered to measure three grinding forces (axial –  $F_x$ , tangential –  $F_y$ , and normal -  $F_z$  in Fig. 1), when the grinding wheel entered the centre of the SiC workpiece. The sampling frequency  $f_s$  was set as 5 kHz.

#### 4. Wear detection

After the four grinding passes, one rather symmetry glazed wear flat is yielded along the circumference of the brass bond grinding wheel (see Fig. 2). The wear flat length is over one third of, but less than one half of the full circumference.

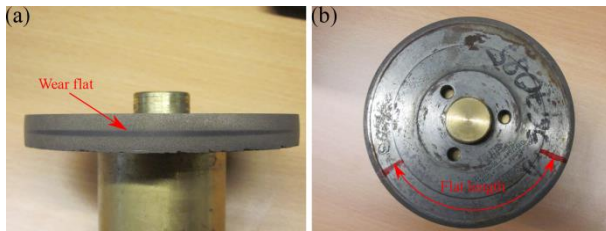


**Figure 2.** Wear flat of brass bond grinding wheel: (a) in the front side with its maximum width and (b) along the wheel circumference.

The waveforms of the tangential and normal grinding forces are presented in four continuous periods, as shown in Fig. 3. The amplitudes of the tangential and normal grinding forces both increase with the grinding passes, which is not enough to estimate the wheel wear in grinding. The two grinding forces act as narrow peaks in all the passes and do not fully occupy each rotation period of the wheel. That means the grinding wheel does not always keep contacting with the SiC workpiece in grinding, which may be caused by the forced vibration of the grinding wheel-workpiece system. It brings more challenges to the wear detection of the brass bond grinding wheel.

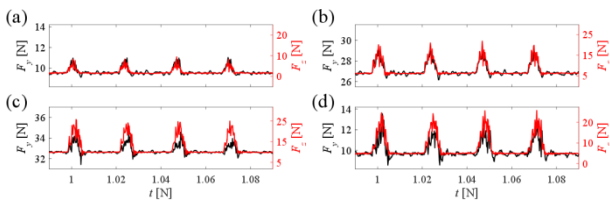


**Figure 3.** Tangential ( $F_y$  in black) and normal ( $F_z$  in red) grinding forces in four periods of: (a) pass 1, (b) pass 2, (c) pass 3, and (d) pass 4.

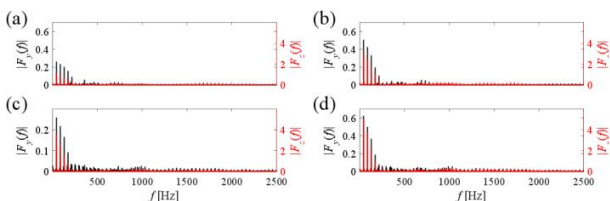


**Figure 4.** Single-sided amplitude spectra of tangential ( $F_y$  in black) and normal ( $F_z$  in red) grinding forces in passes 1-4 corresponding to (a)-(d).

Their single-sided amplitude spectra are shown in Fig. 4, after the four tangential and normal grinding forces are projected

into the frequency domain by using Fourier transform. There are abundant harmonics both in the tangential and normal grinding forces and their amplitudes also raise with the grinding passes. Similar with the waveforms in the time domain, the amplitude spectra of the two grinding forces cannot provide enough intuitive and useful features to detect the wheel wear in grinding.

Figure 5 lists the integrated products of spectral coherences of the tangential and normal grinding forces in the frequency band  $[280, \frac{1}{2}f_s - 280]$  Hz. There are six peaks, i.e. the first six cyclic harmonics, in the cyclic frequency band  $[20\ 280]$  Hz with a fundamental cyclic frequency  $\alpha = 43.3$  Hz, which corresponds to the rotation speed of the spindle 2600 rpm. The six discrete peaks indicate that the tangential and normal grinding forces both present strong second-order cyclostationarity.

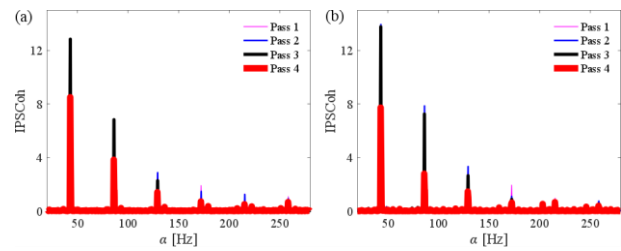


**Figure 5.** Integrated products of spectral coherences of (a) tangential grinding forces and of (b) normal grinding forces in passes 1-4.

Assume that the spindle rotates at the constant speed. Then the grinding wheel rotates over one full circumference  $l$  in the temporal interval  $1/\alpha$ , over  $1/2l$  in  $1/(2\alpha)$ , over  $1/3l$  in  $1/(3\alpha)$ , and so on. Figure 5 (a) and (b) both show that the fourth peak obviously decreases from pass1 to pass 2, but the first three peaks keep constant. The third peak declines from pass 2 to pass 3, while the first two change little. The first three peaks greatly decrease from pass 3 to pass 4.

Comparing the wear flat length in Fig. 2(b) with the variations of the peaks in Fig. 5, it can infer that the wear flat length in each grinding pass determines the behaviours of the peaks in the integrated products of spectral coherences of the tangential and normal forces. The wear flat lengths in passes 1-4 can be estimated to stay in the intervals  $[1/5, 1/4]l$ ,  $[1/4, 1/3]l$ ,  $[1/4, 1/3]l$  and  $[1/3, 1/2]l$ , respectively. Note that the flat length approaches to  $1/4l$  in pass2, but to  $1/3l$  in pass 3.

#### 5. Conclusions

Based on the results in Section 4, two points can be concluded here. First, the grinding forces have strong second-order cyclostationarity, besides many harmonics. Second, the specific peaks in the integrated products of spectral coherences of the tangential and normal forces can be used to estimate the wear flat length of the grinding wheel at the measurement position in each grinding pass.

In future, the performance of the integrated product of spectral coherence will be further verified by other grinding wheels, for example, the resin bond and the ceramic bond diamond grinding wheels.

#### References

- [1] Malkin S and Cook N H 1971 J. Eng. Ind.-T. ASME **93** 1120-28
- [2] Tönshoff H K, Friemuth T and Becker J C 2002 CIRP Ann. **51** 551-71
- [3] Furutani K, Hieu N T, Ohguro N and Nakamura T 2003 Precis. Eng. **27** 9-13
- [4] Antoni J 2009 Mech. Syst. Sig. Process. **23** 987-1036
- [5] Gardner W 1986 IEEE Trans. Acoust. Speech Signal Process. **34** 1111-23
- [6] Urbanek J, Barszcz T and Antoni J 2014 Appl. Acoust. **77** 184-94